Single top quark production at the CERN LHC as a probe of R parity violation

P. Chiappetta
Centre de Physique Théorique, UPR7061, CNRS-Luminy, Case 907, F-13288 Marseille Cedex 9, France

A. Deandrea
Theoretical Physics Division, CERN, CH-1211 Geneva 23, Switzerland

E. Nagy and S. Negroni
Centre de Physique des Particules de Marseille, Université de la Méditerranée, Case 907, F-13288 Marseille Cedex 9, France

G. Polesello
INFN, Sezione di Pavia, via Bassi 6, I-27100 Pavia Italy

J. M. Virey
Institut für Physik, Universität Dortmund, D-44221 Dortmund, Germany
and Centre de Physique Théorique, UPR7061, CNRS-Luminy, Case 907, F-13288 Marseille Cedex 9, France
and Université de Provence, Marseille, France

We investigate the potential of the CERN LHC to probe the R parity violating couplings involving the third generation by considering single top quark production. This study is based on particle level event generation for both signal and background, interfaced to a simplified simulation of the ATLAS detector.

I. INTRODUCTION

The conservation of baryon B and lepton L number is a consequence of the gauge invariance and renormalizability of the standard model. In supersymmetric extensions of the standard model, gauge invariance and renormalizability do not imply baryon and lepton number conservation. We shall consider in what follows the minimal supersymmetric standard model (MSSM) together with baryon or lepton number violating couplings. These Yukawa-type interactions are often referred to as R-parity violating couplings. They can mediate proton decay to an unacceptable level and for this reason a discrete symmetry R was postulated [1] that acts as 1 on all known particles and as -1 on all the superpartners:

$$R = (-1)^{3B+L+2S} \qquad (1)$$

where S is the spin of the particle. In the MSSM with a conserved R parity the lightest supersymmetric particle (LSP) cannot disintegrate into ordinary particles and is therefore stable. The superpartners can be produced only in pairs so that one needs usually to wait for high energy colliders.

In models [2] not constrained by the *ad hoc* imposition of R parity one can still avoid proton decay and the experimental signatures can be quite interesting: single production of supersymmetric particles and modification of standard decays and cross sections due to the exchange of these sparticles, which could be observed at lower energies compared to the R-parity conserving model. In the following we shall investigate top quark production taking into account R-parity violating effects. The top quark being heavy with a mass close to the electroweak symmetry breaking scale, it is believed to be more sensitive to new physics than other quarks.

The mechanism we plan to study is single top quark production at the CERN Large Hadron Collider (LHC), which is complementary to top quark pair production and reliably well known in the standard model.

Two basic ways to probe new physics can be investigated. The first one is a model independent analysis, in which the effects of new physics appear as new terms in an effective Lagrangian describing the interactions of the third family with gauge bosons and Higgs bosons [3–5]. The effects due to the interactions between quarks and gauge bosons will be visible at the CERN e^+e^- collider LEP2, e^+e^- next linear colliders and the Fermilab Tevatron whereas dimension-6 CP violating operators affect the transverse polarization asymmetry of the top quark. The second way is to consider a new theory which contains the standard model at low energies. A possible framework is supersymmetry. In the minimal supersymmetric model with R parity conservation, the single top quark production at Tevatron is enhanced by a few percent due to gluino, squark, Higgs boson, chargino and neutralino corrections, the magnitude being sensitive to $\tan\beta$ [6]. The decays $t \to cV$ with $V = g, Z, \gamma$, which are small in magnitude in the standard model (BR $\simeq 10^{-10}$–10^{-12}), may be enhanced by a few orders of magnitude in the MSSM [7]. If the top squark and the charged Higgs boson are light enough, new top quark decays are possible [8]. Our purpose is to investigate the effects of R parity violation. The superpotential contains three types of new terms:

$$W_R = \lambda_{ijk} L_i L_j \bar{E}_k + \lambda'_{ijk} L_i Q_j \bar{D}_k + \lambda''_{ijk} \bar{U}_i \bar{D}_j \bar{D}_k, \qquad (2)$$

the first two terms violating the leptonic number and the last the baryonic one. Here L and E are isodoublet and isosinglet lepton, Q and D are isodoublet and isosinglet quark super-

fields, and the indices i, j and k take values for the three lepton and quark families. In the following we shall assume that R-parity violation arises from one of these terms only.

The feasibility of single top quark production via squark and slepton exchanges to probe several combinations of R parity violating couplings at hadron colliders has been studied [9–11]. The LHC is better at probing the B violating couplings λ'' whereas the Tevatron and the LHC have a similar sensitivity to λ' couplings. We perform a complete and detailed study including for the signal all channels using a Monte Carlo generator based on PYTHIA 6.1 [12], taking into account all the backgrounds and including the ATLAS detector response using ATLFAST 2.0 [13].

The paper is organized as follows. Section II is devoted to an evaluation of the different subprocesses contributing to single top quark production (standard model, squark, slepton and charged Higgs boson exchanges). The potential of the LHC to discover or put limits on R-parity violating interactions is given in Sec. III.

II. SUBPROCESSES CONTRIBUTING TO SINGLE TOP QUARK PRODUCTION

The R-parity violating parts of the Lagrangian that contribute to single top quark production are

$$L_{\not R} = \lambda'_{ijk} \tilde{e}^i_L \bar{d}^k_R u^j_L - \lambda''_{ijk} (\tilde{d}^k_R \bar{u}^i_L d^j_L + \tilde{d}^j_R (\bar{d}^k_L)^c u^i_L) + \text{H.c.} \quad (3)$$

The superscript c corresponds to charge conjugation. There are altogether 27 and 9 λ'_{ijk} and λ''_{ijk} Yukawa couplings,

respectively. The most suppressed couplings are λ'_{111}, λ'_{133}, λ''_{112}, λ''_{113} (see [14] for detailed up to date reviews of the existing bounds). In order to fix the kinematical variables, the reaction we consider is

$$u_i(p_1) + d_j(p_2) \rightarrow t(p_3) + b(p_4), \quad (4)$$

the p_k being the 4-momenta of the particles and the indices i and j refer to the generations of the u and d-type quarks.

We first discuss valence-valence (VV) or sea-sea (SS) subprocesses (this notation refers to proton-proton collisions at the LHC, but the calculation is valid in general). The SM squared amplitude due to W exchange in the $\hat{u}$ channel[1] is suppressed by the Kobayashi-Maskawa matrix elements $V_{u_i b} V_{t d_j}$:

$$|M^{VV}_{WW}|^2 = g^4 |V_{u_i b}|^2 |V_{t d_j}|^2 \frac{1}{(\hat{u} - m_W^2)^2 + m_W^2 \Gamma_W^2} p_1 \cdot p_2 p_3 \cdot p_4, \quad (5)$$

where g, m and Γ denote the weak coupling constant, the mass and the width of the exchanged particle. The $H^\pm$ exchange in the $\hat{u}$ channel is included in the calculation but numerically suppressed by the quark masses and the mixing matrix elements for the charged Higgs sector $K_{u_i b} K_{t d_j}$ (under the assumption $K = V$),

$$|M^{VV}_{H^\pm H^\pm}|^2 = \frac{g^4}{16 m_W^4} |K_{u_i b}|^2 |K_{t d_j}|^2 \frac{1}{(\hat{u} - m_{H^\pm}^2)^2 + m_{H^\pm}^2 \Gamma_{H^\pm}^2} [(v_{b u_i}^2 + a_{b u_i}^2) p_1 \cdot p_4 + (v_{b u_i}^2 - a_{b u_i}^2) m_b m_{u_i}]$$
$$\times [(v_{d_j t}^2 + a_{d_j t}^2) p_2 \cdot p_3 + (v_{d_j t}^2 - a_{d_j t}^2) m_{d_j} m_t], \quad (6)$$

where v_{ud} and a_{ud} are respectively the vector and axial vector couplings of $H^\pm$ to quarks:

$$v_{ud} = m_d \tan\beta + m_u \cot\beta \quad a_{ud} = m_d \tan\beta - m_u \cot\beta. \quad (7)$$

The interference term between the W and $H^\pm$ is

$$2\,\text{Re}(M^{VV}_{WH^\pm}) = -\frac{g^4}{8 m_W^2} |V_{u_i b}| |V_{t d_j}| |K_{u_i b}| |K_{t d_j}| \frac{(\hat{u} - m_W^2)(\hat{u} - m_{H^\pm}^2) + m_W \Gamma_W m_{H^\pm} \Gamma_{H^\pm}}{[(\hat{u} - m_W^2)^2 + m_W^2 \Gamma_W^2][(\hat{u} - m_{H^\pm}^2)^2 + m_{H^\pm}^2 \Gamma_{H^\pm}^2]}$$
$$\times [(v_{b u_i} + a_{b u_i})(v_{d_j t} + a_{d_j t}) m_b m_{d_j} p_1 \cdot p_3 + (v_{b u_i} + a_{b u_i})(v_{d_j t} - a_{d_j t}) m_b m_t p_1 \cdot p_2$$
$$+ (v_{b u_i} - a_{b u_i})(v_{d_j t} + a_{d_j t}) m_{u_i} m_{d_j} p_3 \cdot p_4 + (v_{b u_i} - a_{b u_i})(v_{d_j t} - a_{d_j t}) m_{u_i} m_t p_2 \cdot p_4]. \quad (8)$$

The scalar slepton exchange in the $\hat{u}$ channel is taken into account but appears to be suppressed within our assumptions on the λ' couplings (see below):

---

[1]The caret refers to the usual Mandelstam variables for the process at the parton level.

$$|M^{VV}_{\tilde{e}^k_L \tilde{e}^k_L}|^2 = \lambda'^2_{ki3} \lambda'^2_{k3j} \frac{1}{(\hat{u} - m^2_{\tilde{e}^k_L})^2 + m^2_{\tilde{e}^k_L} \Gamma^2_{\tilde{e}^k_L}} p_1 \cdot p_4 p_2 \cdot p_3 .$$

(9)

The interference term between scalar slepton and W reads

$$2 \mathcal{R}e(M^{VV}_{W \tilde{e}^k_L}) = -g^2 |V_{u_i b}||V_{td_j}| \lambda'_{ki3} \lambda'_{k3j} \frac{(\hat{u} - m^2_W)(\hat{u} - m^2_{\tilde{e}^k_L}) + m_W \Gamma_W m_{\tilde{e}^k_L} \Gamma_{\tilde{e}^k_L}}{[(\hat{u} - m^2_W)^2 + m^2_W \Gamma^2_W][(\hat{u} - m^2_{\tilde{e}^k_L})^2 + m^2_{\tilde{e}^k_L} \Gamma^2_{\tilde{e}^k_L}]} m_{d_j} m_b p_1 \cdot p_3 .$$

(10)

The interference term between scalar slepton and $H^\pm$, which is suppressed, reads

$$2 \text{Re}(M^{VV}_{\tilde{e}^k_L H^\pm}) = \frac{g^2}{4m^2_W} \lambda'_{ki3} \lambda'_{k3j} |K_{u_i b}||K_{td_j}| \frac{(\hat{u} - m^2_{H^\pm})(\hat{u} - m^2_{\tilde{e}^k_L}) + m_{H^\pm} \Gamma_{H^\pm} m_{\tilde{e}^k_L} \Gamma_{\tilde{e}^k_L}}{[(\hat{u} - m^2_{H^\pm})^2 + m^2_{H^\pm} \Gamma^2_{H^\pm}][(\hat{u} - m^2_{\tilde{e}^k_L})^2 + m^2_{\tilde{e}^k_L} \Gamma^2_{\tilde{e}^k_L}]}$$

$$\times [(v_{bu_i} + a_{bu_i})(v_{d_jt} + a_{d_jt}) p_1 \cdot p_4 p_2 \cdot p_3 + (v_{bu_i} + a_{bu_i})(v_{d_jt} - a_{d_jt}) m_{d_j} m_t p_1 \cdot p_4$$

$$+ (v_{bu_i} - a_{bu_i})(v_{d_jt} + a_{d_jt}) m_{u_i} m_b p_2 \cdot p_3 + (v_{bu_i} - a_{bu_i})(v_{d_jt} - a_{d_jt}) m_{u_i} m_{d_j} m_b m_t].$$

(11)

The down type squark exchange in the $\hat{s}$-channel squared amplitude is dominant and given by

$$|M^{VV}_{\tilde{d}^k_R \tilde{d}^k_R}|^2 = \frac{4}{3} 16 \lambda''^2_{ijk} \lambda''^2_{33k} \frac{1}{(\hat{s} - m^2_{\tilde{d}^k_R})^2 + m^2_{\tilde{d}^k_R} \Gamma^2_{\tilde{d}^k_R}} p_1 \cdot p_2 p_3 \cdot p_4 .$$

(12)

The corresponding interference terms are

$$2 \text{Re}(M^{VV}_{W \tilde{d}^k_R}) = -\frac{2}{3} 8 g^2 |V_{u_i b}||V_{td_j}| \lambda''_{ijk} \lambda''_{33k} \frac{(\hat{u} - m^2_W)(\hat{s} - m^2_{\tilde{d}^k_R}) + m_W \Gamma_W m_{\tilde{d}^k_R} \Gamma_{\tilde{d}^k_R}}{[(\hat{u} - m^2_W)^2 + m^2_W \Gamma^2_W][(\hat{s} - m^2_{\tilde{d}^k_R})^2 + m^2_{\tilde{d}^k_R} \Gamma^2_{\tilde{d}^k_R}]} p_1 \cdot p_2 p_3 \cdot p_4$$

(13)

and

$$2 \text{Re}(M^{VV}_{\tilde{d}^k_R H^\pm}) = \frac{2}{3} \frac{g^2}{2m^2_W} \lambda''_{ijk} \lambda''_{33k} |K_{u_i b}||K_{td_j}| \frac{(\hat{u} - m^2_{H^\pm})(\hat{s} - m^2_{\tilde{d}^k_R}) + m_{H^\pm} \Gamma_{H^\pm} m_{\tilde{d}^k_R} \Gamma_{\tilde{d}^k_R}}{[(\hat{u} - m^2_{H^\pm})^2 + m^2_{H^\pm} \Gamma^2_{H^\pm}][(\hat{s} - m^2_{\tilde{d}^k_R})^2 + m^2_{\tilde{d}^k_R} \Gamma^2_{\tilde{d}^k_R}]}$$

$$\times [(v_{bu_i} + a_{bu_i})(v_{d_jt} + a_{d_jt}) m_b m_{d_j} p_1 \cdot p_3 + (v_{bu_i} + a_{bu_i})(v_{d_jt} - a_{d_jt}) m_b m_t p_1 \cdot p_2$$

$$+ (v_{bu_i} - a_{bu_i})(v_{d_jt} + a_{d_jt}) m_{u_i} m_{d_j} p_3 \cdot p_4 + (v_{bu_i} - a_{bu_i})(v_{d_jt} - a_{d_jt}) m_{u_i} m_t p_2 \cdot p_4].$$

(14)

Let us now take into account the subprocesses involving valence-sea (VS) quarks. The SM squared amplitude due to W exchange in the $\hat{s}$ channel, being proportional to $(V_{u_i d_j} V_{tb})^2$, is dominant for quarks of the same generation. It reads

$$|M^{VS}_{WW}|^2 = g^4 |V_{u_i d_j}|^2 |V_{tb}|^2 \frac{1}{(\hat{s} - m^2_W)^2 + m^2_W \Gamma^2_W} p_1 \cdot p_4 p_2 \cdot p_3 .$$

(15)

The charged Higgs contribution in the $\hat{s}$ channel is suppressed by the quark masses of the initial state. The squared amplitude is

$$|M^{VS}_{H^\pm H^\pm}|^2 = \frac{g^4}{16m^4_W} |K_{u_i d_j}|^2 |K_{tb}|^2 \frac{1}{(\hat{s} - m^2_{H^\pm})^2 + m^2_{H^\pm} \Gamma^2_{H^\pm}} \times [(v^2_{d_ju_i} + a^2_{d_ju_i}) p_1 \cdot p_2 - (v^2_{d_ju_i} - a^2_{d_ju_i}) m_{d_j} m_{u_i}]$$

$$\times [(v^2_{bt} + a^2_{bt}) p_3 \cdot p_4 - (v^2_{bt} - a^2_{bt}) m_b m_t].$$

(16)

The interference term between W and $H^\pm$ is

$$2\,\mathrm{Re}(M_{WH^\pm}^{VS}) = -\frac{g^4}{8m_W^2}|V_{u_id_j}||V_{tb}||K_{u_id_j}||K_{tb}|\frac{(\hat{s}-m_W^2)(\hat{s}-m_{H^\pm}^2)+m_W\Gamma_W m_{H^\pm}\Gamma_{H^\pm}}{[(\hat{s}-m_W^2)^2+m_W^2\Gamma_W^2][(\hat{s}-m_{H^\pm}^2)^2+m_{H^\pm}^2\Gamma_{H^\pm}^2]}$$

$$\times[(v_{d_ju_i}+a_{d_ju_i})(v_{bt}+a_{bt})m_bm_{d_j}p_1\cdot p_3 - (v_{d_ju_i}+a_{d_ju_i})(v_{bt}-a_{bt})m_{d_j}m_t p_1\cdot p_4$$

$$-(v_{d_ju_i}-a_{d_ju_i})(v_{bt}+a_{bt})m_bm_{u_i}p_2\cdot p_3 + (v_{d_ju_i}-a_{d_ju_i})(v_{bt}-a_{bt})m_{u_i}m_t p_2\cdot p_4]. \tag{17}$$

Concerning R parity violating terms, slepton exchange in the $\hat{s}$ channel and down type squark exchange in the $\hat{u}$ channel contribute

$$|M_{\tilde{e}_L^k\tilde{e}_L^k}^{VS}|^2 = \lambda_{kij}'^2\cdot\lambda_{k33}'^2\frac{1}{(\hat{s}-m_{\tilde{e}_L^k}^2)^2+m_{\tilde{e}_L^k}^2\Gamma_{\tilde{e}_L^k}^2}p_1\cdot p_2 p_3\cdot p_4$$

$$|M_{\tilde{d}_R^k\tilde{d}_R^k}^{VS}|^2 = \frac{4}{3}16\lambda_{i3k}''^2\lambda_{3jk}''^2\frac{1}{(\hat{u}-m_{\tilde{d}_R^k}^2)^2+m_{\tilde{d}_R^k}^2\Gamma_{\tilde{d}_R^k}^2}p_1\cdot p_4 p_2\cdot p_3. \tag{18}$$

The interference terms involving the scalar lepton are

$$2\,\mathrm{Re}(M_{W\tilde{e}_L^k}^{VS}) = -g^2|V_{u_id_j}||V_{tb}|\lambda_{kij}'\lambda_{k33}'\frac{(\hat{s}-m_W^2)(\hat{s}-m_{\tilde{e}_L^k}^2)+m_W\Gamma_W m_{\tilde{e}_L^k}\Gamma_{\tilde{e}_L^k}}{[(\hat{s}-m_W^2)^2+m_W^2\Gamma_W^2][(\hat{s}-m_{\tilde{e}_L^k}^2)^2+m_{\tilde{e}_L^k}^2\Gamma_{\tilde{e}_L^k}^2]}m_d m_b p_1\cdot p_3 \tag{19}$$

and

$$2\,\mathrm{Re}(M_{\tilde{e}_L^kH^\pm}^{VS}) = \frac{g^2}{4m_W^2}\lambda_{kij}'\lambda_{k33}'|K_{u_id_j}||K_{tb}|\frac{(\hat{s}-m_{H^\pm}^2)(\hat{s}-m_{\tilde{e}_L^k}^2)+m_{H^\pm}\Gamma_{H^\pm}m_{\tilde{e}_L^k}\Gamma_{\tilde{e}_L^k}}{[(\hat{s}-m_{H^\pm}^2)^2+m_{H^\pm}^2\Gamma_{H^\pm}^2][(\hat{s}-m_{\tilde{e}_L^k}^2)^2+m_{\tilde{e}_L^k}^2\Gamma_{\tilde{e}_L^k}^2]}$$

$$\times[(v_{d_ju_i}+a_{d_ju_i})(v_{bt}+a_{bt})p_1\cdot p_2 p_3\cdot p_4 - (v_{d_ju_i}+a_{d_ju_i})(v_{bt}-a_{bt})m_t m_b p_1\cdot p_2$$

$$-(v_{d_ju_i}-a_{d_ju_i})(v_{bt}+a_{bt})m_{d_j}m_{u_i}p_3\cdot p_4 + (v_{d_ju_i}-a_{d_ju_i})(v_{bt}-a_{bt})m_{u_i}m_{d_j}m_b m_t]. \tag{20}$$

The interference terms involving the scalar quark are

$$2\,\mathrm{Re}(M_{W\tilde{d}_R^k}^{VS}) = -\frac{2}{3}8g^2|V_{u_id_j}||V_{tb}|\lambda_{i3k}''\lambda_{3jk}''\frac{(\hat{s}-m_W^2)(\hat{u}-m_{\tilde{d}_R^k}^2)+m_W\Gamma_W m_{\tilde{d}_R^k}\Gamma_{\tilde{d}_R^k}}{[(\hat{s}-m_W^2)^2+m_W^2\Gamma_W^2][(\hat{u}-m_{\tilde{d}_R^k}^2)^2+m_{\tilde{d}_R^k}^2\Gamma_{\tilde{d}_R^k}^2]}p_1\cdot p_4 p_2\cdot p_3 \tag{21}$$

and

$$2\,\mathrm{Re}(M_{\tilde{d}_R^kH^\pm}^{VS}) = \frac{2}{3}\frac{g^2}{2m_W^2}\lambda_{i3k}''\lambda_{3jk}''|K_{u_id_j}||K_{tb}|\frac{(\hat{s}-m_{H^\pm}^2)(\hat{u}-m_{\tilde{d}_R^k}^2)+m_{H^\pm}\Gamma_{H^\pm}m_{\tilde{d}_R^k}\Gamma_{\tilde{d}_R^k}}{[(\hat{s}-m_{H^\pm}^2)^2+m_{H^\pm}^2\Gamma_{H^\pm}^2][(\hat{u}-m_{\tilde{d}_R^k}^2)^2+m_{\tilde{d}_R^k}^2\Gamma_{\tilde{d}_R^k}^2]}$$

$$\times[(v_{d_ju_i}+a_{d_ju_i})(v_{bt}+a_{bt})m_bm_{d_j}p_1\cdot p_3 - (v_{d_ju_i}+a_{d_ju_i})(v_{bt}-a_{bt})m_{d_j}m_t p_1\cdot p_4$$

$$-(v_{d_ju_i}-a_{d_ju_i})(v_{bt}+a_{bt})m_bm_{u_i}p_2\cdot p_3 + (v_{d_ju_i}-a_{d_ju_i})(v_{bt}-a_{bt})m_{u_i}m_t p_2\cdot p_4]. \tag{22}$$

The dominant terms are the squared amplitude due to $\tilde{e}$ exchange, and for initial quarks of the same generation ($i=j$), the interference between W and $\tilde{d}$. The result is sensitive to the interference term only if the product of λ'' couplings is large (around 10^{-1}). For subprocesses involving quarks of different generations in the initial state the situation is more complex and all amplitudes have to be taken into account.

The resonant $\hat{s}$ channel processes have been studied in

TABLE I. Total cross section in pb for squark exchange in the $\hat{s}$ channel for a squark of mass of 600 GeV assuming $\Gamma_R = 0.5$ GeV.

Initial partons	cd	cs	ub		cb
Exchanged particle	$\tilde{s}$	$\tilde{d}$	$\tilde{s}$	$\tilde{d}$	$\tilde{s}$
Couplings	$\lambda''_{212}\lambda''_{332}$	$\lambda''_{212}\lambda''_{331}$	$\lambda''_{132}\lambda''_{332}$	$\lambda''_{231}\lambda''_{331}$	$\lambda''_{232}\lambda''_{332}$
Cross section in pb	3.98	1.45	5.01	0.659	

[11], for first family up and down quarks. For the B-violating couplings, the study of $\hat{s}$ channels $cd \to \tilde{s}$ and $cs \to \tilde{d}$ can also be found in [11]. The $\hat{u}$ diagram has been studied at the Tevatron for the first family of up and down quarks [10].

In the present paper we have improved previous calculations for LHC because we have included all contributions to single top quark production. Since the dominant terms are those considered in the literature, our complete evaluation validates the approximations done in previous papers.

III. DETECTION OF SINGLE TOP QUARK PRODUCTION THROUGH R-PARITY VIOLATION AT THE LHC

We have carried out the feasibility study to detect single top quark production through R-parity violation at the LHC by measuring the $l\nu bb$ final state using the following procedure.

First, we have implemented the partonic $2 \to 2$ cross sections calculated using Eqs. (5)–(22) in the PYTHIA event generator. Providing PYTHIA with the flavor and the momenta of the initial partons using a given parton distribution function (PDF)[2] it then generates complete final states including initial and final state radiations and hadronization.

The generated events were implemented in ATLFAST to simulate the response of the ATLAS detector. In particular, isolated electrons and photons were smeared with the detector resolution in the pseudo-rapidity range of $|\eta| < 2.5$. In the same way and the same η region the measured parameters of the isolated and non-isolated muons were simulated. Finally, a simple fixed cone algorithm (of radius $R = 0.4$) was used to reconstruct the parton jets. The minimum transverse energy of a jet was set at 15 GeV. According to the expected b-tagging performance of the ATLAS detector [15] for low luminosity at the LHC we have assumed a 60% b-tag efficiency for a factor 100 of rejection against light jets.

The same procedure was applied to the SM background

with the exception that we used besides PYTHIA also the ONE-TOP [16] event generator.

The integrated luminosity for 1 y at low luminosity at the LHC is taken to be 10 fb^{-1}.

The number of signal events depends on the mass and the width of the exchanged sparticle and on the value of the Yukawa couplings (see Sec. II). We assume that only one type of Yukawa coupling is nonzero; i.e., either sleptons ($\lambda' \neq 0$) or squarks ($\lambda'' \neq 0$) are exchanged. The width of the the exchanged sparticle is a sum of the widths due to R-parity conserving and R-parity violating decays:

$$\Gamma_{tot} = \Gamma_R + \Gamma_{\not R} \tag{23}$$

where $\Gamma_{\not R}$ is given by

$$\Gamma_{\not R}(\tilde{q}_R^i \to q^j q^k) = \frac{(\lambda''_{ijk})^2}{2\pi} \frac{(M_{\tilde{q}_R^i}^2 - M_{top}^2)^2}{M_{\tilde{q}_R^i}^3} \tag{24}$$

for the squarks, and it is given by

$$\Gamma_{\not R}(\tilde{l}_L^i \to q^j \bar{q}^k) = \frac{3(\lambda'_{ijk})^2}{16\pi} \frac{(M_{\tilde{l}_L^i}^2 - M_{top}^2)^2}{M_{\tilde{l}_L^i}^3} \tag{25}$$

for the sleptons. The number of signal events depends also on the flavor of the initial partons through their PDF. In Table I we display the total cross section values for different initial parton flavors in the case of exchanged squarks of mass of 600 GeV and of R-parity conserving width $\Gamma_R = 0.5$ GeV. We took for all $\lambda'' = 10^{-1}$, which yields a natural width of the squark which is smaller than the experimental resolution. Table II contains the same information for slepton exchange ($\lambda' = 10^{-1}$, for a slepton of mass of 250 GeV and

TABLE II. Total cross section in pb for slepton exchange in the $\hat{s}$ channel for a slepton of mass of 250 GeV assuming $\Gamma_R = 0.5$ GeV.

Initial partons	$u\bar{d}$	$u\bar{s}$	$c\bar{d}$	$c\bar{s}$	$u\bar{b}$	$c\bar{b}$
Couplings	$\lambda'_{11k}\lambda'_{k33}$	$\lambda'_{12k}\lambda'_{k33}$	$\lambda'_{21k}\lambda'_{k33}$	$\lambda'_{22k}\lambda'_{k33}$	$\lambda'_{13k}\lambda'_{k33}$	$\lambda'_{23k}\lambda'_{k33}$
Cross section in pb	7.05	4.45	2.31	1.07	2.64	0.525

---

[2]We have used the CTEQ3L PDF. We checked that the use of different sets of parton distribution functions induces an uncertainty in the results which is around the percent level. This in no way affects our conclusions.

TABLE III. $\sigma \times$ branching ratio for backgrounds.

Background	$\sigma \times$ BR (pb)
$W*$	2.2
Gluon fusion	54
Wt	17
$t\bar{t}$	246
Wbb	66.6
Wjj	440

a width of $\Gamma_R = 0.5$ GeV). Other processes are not quoted because the small value of the limits of their couplings prevents their detection.

In order to study the dependence of the signal on the mass and the width of the exchanged particle we have fixed the couplings to 10^{-1} and have chosen three different masses for the exchanged squarks: 300, 600 and 900 GeV, respectively. For each mass value we have chosen two different Γ_R: 0.5 and 20 GeV, respectively. For the first case $\Gamma_{\tilde{k}}$ dominates, whereas in the last one, when $\Gamma_{tot} \approx \Gamma_R$, the single top quark production cross section decreases by a factor of ~ 10. We have considered here the ub parton initial state, since this has the highest cross section value. Besides, we have also generated events with a cd initial partonic state and an exchanged $\tilde{s}$ quark of mass of 300 GeV, for comparison with the simulation presented in Ref. [11].

In order to study the dependence on the parton initial state we have fixed the mass of the exchanged squark to 600 GeV and its width with $\Gamma_R = 0.5$ GeV and varied the initial state according to the first line of Table I.

Finally, for the exchanged sleptons we have studied only one case, namely the $u\bar{d}$ initial state with a mass and width of the exchanged slepton of 250 GeV and 0.5 GeV, respectively. In each case we have generated about 10^5 signal events.

The different types of background considered are listed in Table III together with their estimated cross sections. The

FIG. 2. Invariant mass distribution of $l\nu bb$ combination for the signal and backgrounds (dashed histogram) after 3 y of LHC run at low luminosity. The signal corresponds to an exchanged $\tilde{s}$ quark of 600 GeV mass and 0.5 GeV width. The initial partons are ub and the λ'' couplings are set to 10^{-1}.

irreducible backgrounds are single top quark production through a virtual W (noted $W*$), or through W-gluon fusion. W-gluon fusion is the dominant process (for a detailed study see [17]). A Wbb final state can be obtained either in direct production or through Wt or $t\bar{t}$ production. Finally, the reducible background consists of W-nj events where two of the jets are misidentified as b-jets.

We have used the ONETOP [16] event generator to simulate the W-gluon fusion process. For the other backgrounds we have used PYTHIA. We have generated from 1000 ($W*$) to several 1×10^6 events ($t\bar{t}$) depending on the importance of the background.

The separation of the signal from the background is based on the presence of a resonant structure of the tb final state in the case of the signal. The background does not show such a structure as it is illustrated in Fig. 1.
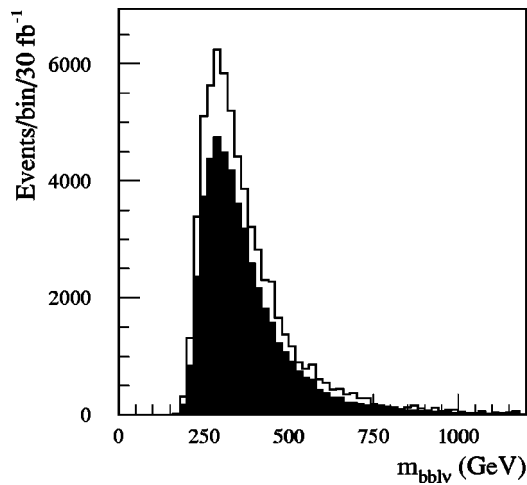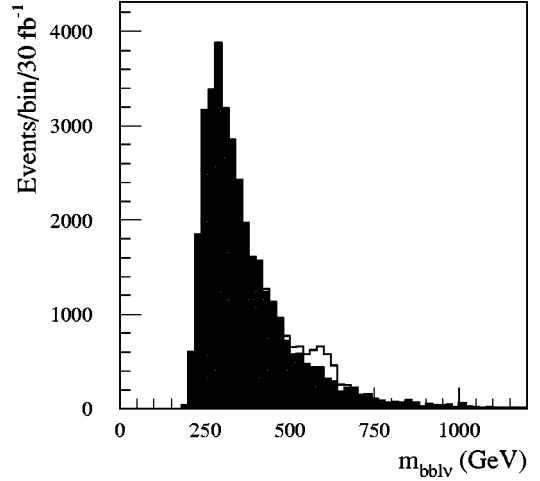

FIG. 1. Invariant mass distribution of $l\nu bb$ for the backgrounds after 3 y at LHC at low luminosity. The $t\bar{t}$ background dominates (dashed histogram).
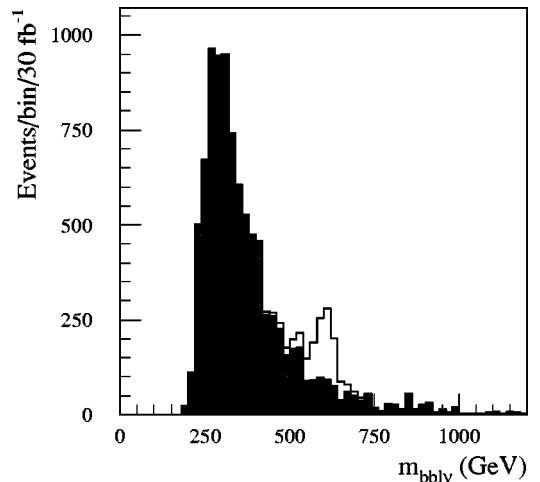

FIG. 3. Invariant mass distribution of $l\nu bb$ for the signal and backgrounds (dashed histogram) after 3 y at LHC at low luminosity after having applied the cuts.

TABLE IV. Limits for the values of the $\lambda''_{132}\lambda''_{332}$ Yukawa couplings for an integrated luminosity of 30 fb^{-1}. For the other quantities see the text. Current limit is 6.25×10^{-1}.

$m_{\tilde{s}}$ (GeV)	300		600		900	
Γ_R (GeV)	0.5	20	0.5	20	0.5	20
N_s	6300	250	703	69	161	22
N_b	4920	5640	558	1056	222	215
Γ_{expt} (GeV)	24.3	30.5	37.5	55.6	55.4	62.1
Limits on $\lambda''\times\lambda''$	2.36×10^{-3}	1.21×10^{-2}	4.10×10^{-3}	1.51×10^{-2}	6.09×10^{-3}	2.09×10^{-2}

In the process to reconstruct the tb final state first we reconstruct the top quark. The top quark can be reconstructed from the W and from one of the b quarks in the final state, requiring that their invariant mass satisfy

$$150\leq M_{Wb}\leq200 \text{ GeV}.$$

The W is in turn reconstructed from either of the two decay channels:

$$W\to u\bar{d}$$

$$W\to l\nu.$$

Here we have considered only the latter case which gives a better signature due to the presence of a high p_t lepton and missing energy. The former case suffers from multi-jet event backgrounds. As we have only one neutrino, its longitudinal momentum can be reconstructed by using the W and top mass constraints. The procedure used is the following:

(i) We keep events with two b-jets of $p_t\geq40$ GeV, with one lepton of $p_t\geq25$ GeV, with $E_t^{miss}\geq35$ GeV and with a jet multiplicity ≤3.

(ii) We reconstruct the longitudinal component (p_z) of the neutrino by requiring $M_{l\nu}=M_W$. This leads to an equation with twofold ambiguity on p_z.

(iii) More than 80% of the events have at least one solution for p_z. In case of two solutions, we calculate $M_{l\nu b}$ for each of the two b jets and we keep the p_z that minimizes $|M_{top}-M_{l\nu b}|$.

(iv) We keep only events where $150\leq M_{l\nu b}\leq200$ GeV.

Next, the reconstructed top quark is combined with the b quark not taking part in the top reconstruction. An example of the invariant mass distribution of the tb final state is shown in Fig. 2.

In order to reduce the the $t\bar{t}$ background to a manageable level, we need to apply a strong jet veto on the third jet by requiring that its p_t should be ≤20 GeV.

The invariant mass distribution of the tb final state after having applied this cut is shown in Fig. 3. The signal to background ratio is clearly increased in comparison to Fig. 2.

Once an indication for a signal is found, we count the number of signal (N_s) and background (N_b) events in an interval corresponding to 2 standard deviations around the signal peak for an integrated luminosity of 30 fb^{-1}. Then we rescale the signal peak by a factor α such that
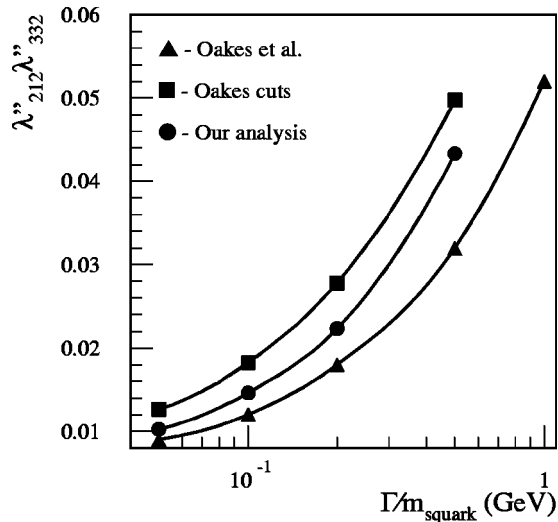
$$N_s/\sqrt{N_b}=5.$$

FIG. 4. Sensitivity limits for the values of the $\lambda''_{212}\lambda''_{332}$ Yukawa couplings we obtain for the cd initial state at the LHC after 1 y with low luminosity, for an exchanged $\tilde{s}$ quark of mass of 300 GeV (circles). The result obtained by Oakes *et al.* is also shown (triangles). The squares indicate a result obtained by applying the cuts used by Oakes *et al.* on our sample.
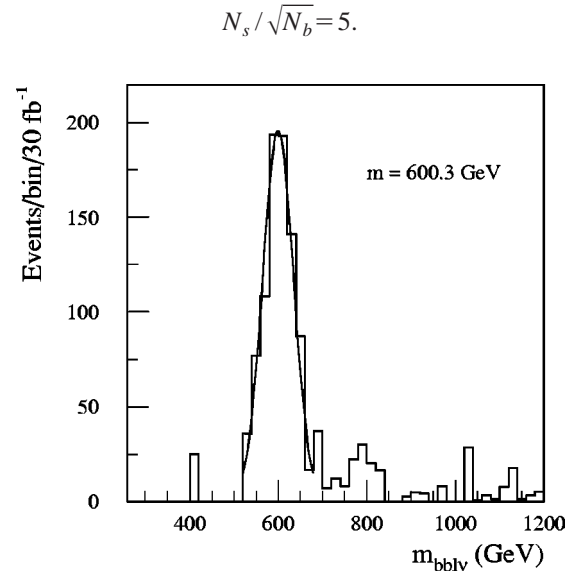

FIG. 5. The background subtracted mass distribution fitted with a Gaussian in case of an exchanged $\tilde{s}$ quark of 600 GeV for a ub initial parton state. It corresponds to 3 y of LHC run with low luminosity.

TABLE V. Limits on the Yukawa couplings for an exchanged squark of mass 600 GeV assuming $\Gamma_R = 0.5$ GeV, for an integrated luminosity of 30 fb^{-1}. Current limit is 6.25×10^{-1}.

Initial partons	cd	cs	ub	cb	
Exchanged particle	$\tilde{s}$	$\tilde{d}$	$\tilde{s}$	$\tilde{d}$	$\tilde{s}$
Couplings	$\lambda''_{212}\lambda''_{332}$	$\lambda''_{212}\lambda''_{331}$	$\lambda''_{132}\lambda''_{332}$	$\lambda''_{231}\lambda''_{331}$	$\lambda''_{232}\lambda''_{332}$
N_s	660	236	703	96	
N_b	558	558	558	558	
Γ_{expt} (GeV)	38.5	31.3	37.5	40.1	
Limits on $\lambda'' \times \lambda''$	4.26×10^{-3}	7.08×10^{-3}	4.1×10^{-3}	1.11×10^{-2}	

By definition the scale factor α determines the limit of sensitivity for the lowest value of the λ'' (λ') coupling we can test with the LHC:

$$\lambda''_{ijk} \cdot \lambda''_{lmn} \lesssim 0.01\sqrt{\alpha}.$$

In Table IV we show the limits obtained for the combinations of $\lambda''_{132}\lambda''_{332}$ for different masses and widths of the exchanged $\tilde{s}$ quark. Also shown are the current limits assuming a mass for $\tilde{m}_f = 100$ GeV, the number of signal and background events, as well as the experimentally observable widths of the peak (Γ_{expt}). In Fig. 4 we compare our results with those obtained in Ref. [11] for $m_{\tilde{s}} = 300$ GeV and a cd initial state, using parton-level simulation. We ascribe the lower efficiency of this analysis to the more detailed and realistic detector simulation employed.

In Table V we compile the sensitivity limit of the bilinear combination of the different Yukawa couplings one can obtain after 3 y of LHC run with low luminosity, if the exchanged squark has a mass of 600 GeV. For its width we consider $\Gamma_R = 0.5$ GeV and a component Γ_k given by Eq. (24).

For the exchanged sleptons (cf. Table II) we have calculated the sensitivity limit of the bilinear combination of the different Yukawa couplings only for the most favorable case, i.e. for the $u\bar{d}$ partonic initial state. We obtain 4.63×10^{-3} for the limits on $\lambda'_{11k}\lambda'_{k33}$ (in comparison with the limit of 2.8×10^{-3} obtained by Oakes *et al.*). For those cases where the exchanged squark (slepton) might be discovered at the LHC we have made an estimate on the precision one can determine its mass. For this purpose, we have subtracted the background under the mass peak and fitted a Gaussian curve on the remaining signal. This procedure is illustrated in Fig. 5 for the case of 600 GeV squark mass and ub partonic initial state. For the assumed value of the coupling constant, the error on the mass determination is dominated by the 1% systematic uncertainty on the jet energy scale in ATLAS [15].

IV. CONCLUSIONS

We have studied single top production through *R*-parity violating Yukawa type couplings, at the LHC.

We have considered all $2 \to 2$ partonic processes at the tree level, including interference terms. The calculated $2 \to 2$ partonic cross sections have been implemented in PYTHIA to generate complete particle final states. A fast particle level simulation was used to obtain the response of the ATLAS detector. We have taken into account all important SM backgrounds.

We have studied the signal-to-background ratio as a function of the initial partonic states, the exchanged sparticle mass and width, and of the value of the Yukawa couplings.

At the chosen value of the coupling constants ($\sim 10^{-1}$), significant signal-to-background ratio was obtained only in the $\hat{s}$-channel, in the tb ($l\nu bb$) invariant mass distribution, around the mass of the exchanged sparticle, if

(i) the exchanged sparticle is a squark, and

(ii) its width due to *R*-parity conserving decay is of the order of a GeV.

In this case we obtain a significance of $S = N_s/\sqrt{N_b} > 5$ for the whole mass range investigated (300 – 900 GeV) for an integrated luminosity of 30 fb^{-1}. This means that squarks ($\tilde{d}$ or $\tilde{s}$) with a narrow width might be discovered at the LHC. The experimental mass resolution would allow to measure the squark mass with a precision of $\sim 1\%$.

Conversely, if no single top quark production above the SM expectation is observed at the LHC, after 3 y the experimental limit on the quadratic combination of the λ'' couplings can be lowered by at least one order of magnitude, for narrow width squarks. In the case of slepton exchange significant signal-to-background ratio can be obtained for $u\bar{d}$ partonic initial state, i.e. for the combination of the $\lambda'_{11k}\lambda'_{k33}$ couplings. As a result of the lower rate, as compared to squark exchange, in the absence of a signal, the current limit can be improved only by a factor of 2. The difference between the significance in our study and the one in Ref. [11] can be explained by the different degree of detail in the simulation process.

[1] P. Fayet, Phys. Lett. **69B**, 489 (1977); G. Farrar and P. Fayet, *ibid.* **76B**, 575 (1978).

[2] C. S. Aulakh and R. N. Mohapatra, Phys. Lett. **119B**, 136 (1982); F. Zwirner, *ibid.* **132B**, 103 (1983); L. Hall and M. Suzuki, Nucl. Phys. **B231**, 419 (1984); J. Ellis *et al.*, Phys. Lett. **150B**, 142 (1985); G. Ross and J. Valle, *ibid.* **151B**, 375 (1985); S. Dawson, Nucl. Phys. **B261**, 297 (1985); R. Barbieri and A. Masiero, *ibid.* **B267**, 679 (1986); S. Dimopoulos and L. J. Hall, Phys. Lett. B **207**, 210 (1987); L. E. Ibanez and G. G. Ross, Nucl. Phys. **B368**, 3 (1992); S. Lola, G. G. Ross, Phys. Lett. B **314**, 336 (1993); J. Ellis, S. Lola, and G. G. Ross, Nucl. Phys. **B526**, 115 (1998).

[3] G. J. Gounaris, D. T. Papadamou, and F. M. Renard, Z. Phys. C **76**, 333 (1997).

[4] K. Whisnant, J. M. Yang, B. L. Young, and X. Zhang, Phys. Rev. D **56**, 467 (1997).

[5] J. M. Yang and B. L. Young, Phys. Rev. D **56**, 5907 (1997).

[6] C. S. Li, R. J. Oakes, J. M. Yang, and H. Y. Zhou, Phys. Rev. D **57**, 2009 (1998).

[7] G. Couture, C. Hamzaoui, and H. Konig, Phys. Rev. D **52**, 1713 (1995); J. L. Lopez, D. V. Nanopoulos, and R. Rangarajan, *ibid.* **56**, 3100 (1997); G. Couture, M. Frank, and H. Konig, *ibid.* **56**, 4213 (1997); G. M. de Divitiis, R. Petronzio, and L. Silvestrini, Nucl. Phys. **B504**, 45 (1997).

[8] M. Hosch, R. J. Oakes, K. Whisnant, J. M. Yang, B. L. Young, and X. Zhang, Phys. Rev. D **58**, 034002 (1998); S. Mrenna and C. P. Yuan, Phys. Lett. B **367**, 188 (1996); J. Guasch and J. Sola, *ibid.* **416**, 353 (1998).

[9] H. Dreiner and G. G. Ross, Nucl. Phys. **B365**, 597 (1991).

[10] A. Datta, J. M. Yang, B. L. Young, and X. Zhang, Phys. Rev. D **56**, 3107 (1997).

[11] R. J. Oakes, K. Whisnant, J. M. Yang, B. L. Young, and X. Zhang, Phys. Rev. D **57**, 534 (1998).

[12] T. Sjöstrand, Comput. Phys. Commun. **82**, 74 (1994).

[13] E. Richter-Wąs, D. Froidevaux, and L. Poggioli, ATLAS Internal Note No. Phys-No-79, 1996.

[14] G. Bhattacharyya, Nucl. Phys. B (Proc. Suppl.) **52A**, 83 (1997); H. Dreiner, hep-ph/9707435; in *Perspectives on Supersymmetry*, edited by G. Kane (World Scientific, Singapore, in press; Report of the *R*-parity group of GDR SUSY, hep-ph/9810232, available at http://www.in2p3.fr/susy/ and references therein; B. C. Allanach, A. Dedes, and H. K. Dreiner, Phys. Rev. D **60**, 075014 (1999); B. Allanach *et al.*, in Physics at Run II: Workshop on Supersymmetry/Higgs, Batavia, IL, 1998, hep-ph/9906224.

[15] ATLAS Collaboration, Detector and Physics Performance Technical Design Report No. CERN/LHCC/99-14, ATLAS TDR 14, 1999.

[16] C. P. Yuan, D. Carlson, S. Mrenna, Barringer, B. Pineiro, and R. Brock, and computer code ONETOP, http://www.pa.msu.edu/~brock/atlas-1top/EW-top-programs.html

[17] T. Stelzer, Z. Sullivan, and S. Willenbrock, Phys. Rev. D **58**, 094021 (1998).